



OPEN

Potent effects of dioscin against obesity in mice

There are amendments to this paper

SUBJECT AREAS:
DRUG DEVELOPMENT
NATURAL PRODUCTSMin Liu¹, Lina Xu¹, Lianhong Yin¹, Yan Qi¹, Youwei Xu¹, Xu Han¹, Yanyan Zhao¹, Huijun Sun¹, Jihong Yao¹, Yuan Lin¹, Kexin Liu¹ & Jinyong Peng^{1,2}Received
7 August 2014Accepted
12 December 2014Published
22 January 2015Correspondence and
requests for materials
should be addressed to
J.P.
(jinyongpeng2008@
126.com)¹College of Pharmacy, Dalian Medical University, Western 9 Lvshunnan Road, Dalian 116044, China, ²Research Institute of Integrated Traditional and Western Medicine of Dalian Medical University, Dalian 116044, China.

The mechanisms of the natural product dioscin against non-alcoholic fatty liver disease (NAFLD) are unclear. Thus, the purpose of the present study was to further confirm its effects of prevention and then to elucidate the potential mechanisms underlying its activity in mice. High-fat diet (HFD)-induced C57BL/6J mice and ob/ob mice were used as the experimental models. Serum and hepatic biochemical parameters were determined, and the mRNA and protein expression levels were detected. The results indicated that dioscin alleviated body weight and liver lipid accumulation symptoms, increased oxygen consumption and energy expenditure, and improved the levels of serum and hepatic biochemical parameters. Further investigations revealed that dioscin significantly attenuated oxidative damage, suppressed inflammation, inhibited triglyceride and cholesterol synthesis, promoted fatty acid β -oxidation, down-regulated MAPK phosphorylation levels, and induced autophagy to alleviate fatty liver conditions. Dioscin prevents diet induced obesity and NAFLD by increasing energy expenditure. This agent should be developed as a new candidate for obesity and NAFLD prevention.

Non-alcoholic fatty liver disease (NAFLD), which is considered to be the hepatic manifestation of the metabolic syndrome, represents a spectrum of liver pathology ranging from simple steatosis to serious conditions including steatohepatitis, fibrosis, irreversible cirrhosis, and hepatocellular carcinoma in the absence of alcohol abuse¹. Given its rapidly increasing incidence, NAFLD is now the most common cause of chronic liver disease, with a prevalence of up to 30% in developed countries and nearly 10% in developing nations².

Excessive and inappropriate dietary-fat intake combined with peripheral insulin resistance, continued triglyceride (TG) hydrolysis via lipoprotein lipase, and other genetic alterations in the key lipid metabolic pathways can cause increased blood free-fatty-acid (FFA) and TG levels in liver³. The accumulation of lipids in hepatocytes promotes mitochondrial dysfunction, oxidative stress, and inflammation⁴, thereby leading to lipid metabolism disorders.

At present, the molecular mechanisms of NAFLD have been widely investigated and are progressively being understood. Oxidative stress can induce lipid peroxidation, including hepatic injury and inflammation, and promote the progression toward non-alcoholic steatohepatitis⁵, but some biological molecules, including nuclear factor E2-related factor-2 (Nrf2) and the antioxidative stress enzymes heme oxygenase-1 (HO-1) and superoxide dismutase (SOD), can restore the imbalance of oxidative stress⁶. In addition, oxidative stress also can activate the AMP-activated protein kinase (AMPK) signaling pathway, and activated c-junN-terminal kinase (JNK) and p38 contribute to the increased expression of inflammatory cytokines⁷. In addition, the inflammatory factors TNF- α and IL-1 play primary roles in the pathology of non-alcoholic steatohepatitis by stimulating hepatic lipogenesis and causing hepatic mitochondrial dysfunction and oxidative stress, which induces liver injury⁸. Moreover, reduced NF- κ B and COX-2 activation in the liver also alleviates steatohepatitis⁹.

In addition, autophagy is cellular self-digestion that occurs in eukaryotes and plays an important role in protecting cellular homeostasis and survival by degrading old, unfolded, or damaged organelles and proteins¹⁰. In this process, macroautophagy is one necessary cellular degradation course with major pathophysiological significance¹¹. More importantly, autophagy can regulate intracellular lipid levels by degrading lipid droplets¹².

When fatty acid synthesis is increased and fatty acid metabolism is impaired in the liver, TG levels and various biological molecules involved in TG synthesis are increased¹³. Moreover, increased fatty acid synthesis and total triglyceride (TG) synthesis as well as impaired fatty acid catabolism in the liver are regarded as additional

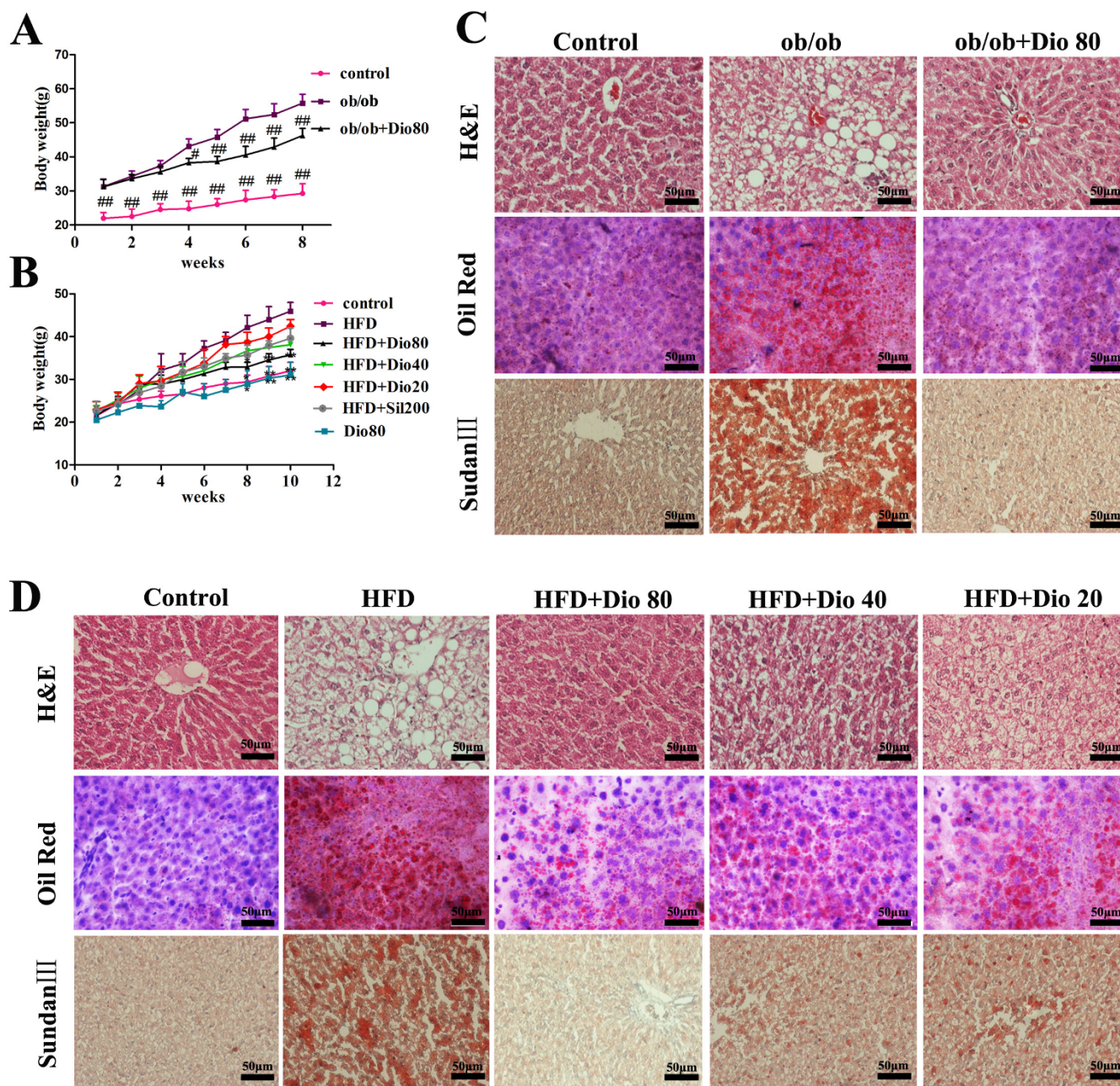


Figure 1 | Effects of dioscin on mouse body weights and histopathological examination results. Effects of dioscin on body weight (A and B) and histopathological examination by H&E, Oil Red O, and Sudan III staining (C and D) in ob/ob and C57BL/6J mice ($\times 400$, magnification). Data are presented as mean \pm SD (n = 8). *p, *p < 0.05 and #p, **p < 0.01 compared with model group.

mechanisms in the pathogenesis of fatty liver injury¹⁴. Thus, chemicals that affect fatty acid synthesis, fatty acid metabolism, or TG synthesis can be used to treat NAFLD.

Currently, NAFLD treatments involve rational diet, exercise, and drugs, including metformin, statins, and fibrates. However, these drugs have some adverse effects or contraindications, and there is still no consensus on the most effective drug therapy¹⁵. Therefore, new candidates with high efficiency and little or no side effects are urgently needed for the treatment of NAFLD.

Traditional Chinese medicines (TCMs) are rich sources of biologically active substances that can be used to prevent human diseases¹⁶. Currently, more and more studies have focused on herbal extracts or natural products, and various herbal products with anti-hyperlipidemic and hepatoprotective effects against NAFLD have

been identified¹⁷. Thus, it is reasonable to develop effective natural products for the treatment of NAFLD.

Dioscin (Dio, shown in Supplemental Figure 1), a natural steroid saponin, widely exists in various herbs¹⁸. Pharmacological studies have demonstrated that dioscin has anti-tumor¹⁹, anti-hyperlipidemic²⁰, and anti-fungal²¹ activities. In our previous studies, dioscin exhibited remarkable protective effects against CCl₄, paracetamol-, and ethanol-induced liver injury^{22–24}, and effects against NAFLD in rats were also identified²⁵. However, the molecular mechanisms of dioscin against NAFLD are still unknown, and the pharmacodynamics of this agent should be further confirmed.

Therefore, the aim of the present work was to further validate the effects of dioscin against NAFLD using two types of animal models, including high-fat diet (HFD) induced-mice and ob/ob mice, and to



Table 1 | The effects of dioscin on the biochemical parameters in ob/ob mice

Parameters	Control	ob/ob	ob/ob + Dio 80
AST (IU/L)	12.89 ± 2.36**	102.62 ± 11.68	55.95 ± 9.62**
ALT (IU/L)	26.91 ± 4.94**	90.25 ± 11.11	55.59 ± 7.63**
Insulin (mIU/L)	15.34 ± 2.19**	32.34 ± 2.49	21.56 ± 2.35**
FFA (μmol/gprot)	42.39 ± 9.91**	255.35 ± 16.64	108.53 ± 20.84**
TC (mmol/L)	9.28 ± 3.38**	89.04 ± 13.71	40.16 ± 5.88**
TG (mmol/L)	123.49 ± 20.98**	341.92 ± 49.01	171.57 ± 35.02**
MDA (U/mgprot)	14.46 ± 3.44**	82.49 ± 10.71	45.05 ± 8.16**
GSH (U/mgprot)	235.31 ± 12.63**	107.24 ± 11.26	201.58 ± 18.75*
SOD (U/mgprot)	23.06 ± 3.95**	8.71 ± 1.60	17.32 ± 4.97**

Data are presented as mean ± SD (n = 8). *p < 0.05, **p < 0.01 compared with model group.

investigate the possible mechanisms related to the anti-NAFLD activity.

Results

Effects of dioscin on ob/ob and HFD-treated mice body weight. As shown in Figure 1A, dioscin (80 mg/kg) administered to ob/ob mice significantly decreased body weight (control, 29.2 ± 2.2 g; ob/ob, 55.6 ± 5.2 g; ob/ob + Dio, 46.5 ± 4.4 g). After feeding C57BL/6J mice a HFD for 10 weeks, the body weights of the animals with HFD diet were significantly increased compared with the mice in control and Dio 80 groups, which were significantly decreased by dioscin (80, 40, and 20 mg/kg) or silymarin (Figure 1B). Therefore, dioscin treatment inhibited the obesity in ob/ob mice and C57BL/6J mice caused by HFD.

Effects of dioscin on hepatic tissue pathology. As shown in Figure 1C–D, the liver histopathology exhibited widespread lipid vacuoles deposited inside the parenchyma cells in ob/ob and C57BL/6J model groups compared with the control groups. However, dioscin-treated groups exhibited fewer microvesicular fatty changes. Oil Red O- and Sudan III-stained sections indicated that the lipid droplets in hepatocytes were significantly increased in ob/ob and C57BL/6J model groups and were obviously decreased by dioscin (80, 40, and 20 mg/kg) with dose-dependent manner.

Effects of dioscin on the biochemical parameters. The effects of dioscin on the serum parameters of ALT, AST, insulin, TC, TG, and the levels of FFA, SOD, MDA, GSH from liver tissue in ob/ob and C57BL/6J mice were investigated. As listed in Tables 1–2, compared with model groups, the increased levels of AST, ALT, insulin, FFA, TC, TG, MDA were all significantly attenuated by dioscin. Meanwhile, the SOD level was markedly elevated by dioscin at the doses of 80, 40 and 20 mg/kg with p < 0.01, and the level of GSH was also elevated by dioscin at the dose of 80 mg/kg with p < 0.05.

Effects of dioscin on blood glucose levels. The levels of fasting blood glucose and OGTT are presented in Figure 2A. The ob/ob and HFD

groups had the highest fasting blood glucose levels which were significantly decreased by dioscin (80 mg/kg) supplementation with p < 0.01 in ob/ob mice and p < 0.05 in HFD mice compared with model. And the blood glucose levels were also highest in model groups after the administration of the glucose overload, which characterized the ob/ob and the HFD obesity groups with the most affected carbohydrate metabolism. The highest peak was observed at 30 min in OGTT, and the glucose levels had significant dose-dependent decreases which were observed in dioscin-treated groups compared with model groups, especially the Dio 80.

Dioscin elevates the energy expenditure of ob/ob mice and HFD mice. As shown in Figure 2B, no difference in food intake for the dioscin-treated groups suggested that the factors other than energy intake contributed to the resistance of weight gain by dioscin. Meanwhile, dioscin also did not change the physical activity of mice, as no obvious change in the locomotor activity was observed between the ob/ob and ob/ob + Dio80, HFD and HFD + Dio80 mice (p > 0.05 vs. the ob/ob and the HFD group, respectively). Therefore, we conducted indirect calorimetric studies to ascertain whether the resistance to weight gain was associated with an increase in energy expenditure. As shown in Figure 2C, the results showed that a significant elevation in energy expenditure in the dioscin-treated mice (p < 0.05 vs. the ob/ob and the HFD group, respectively).

Effects of dioscin on the expression of various proteins related to oxidative stress. The effects of dioscin on the expression of HO-1, Nrf2, GSS, SOD2, and KEAP1 in ob/ob and C57BL/6J mice are presented in Figure 3A. Compared with the model groups, dioscin significantly up-regulated the expression of HO-1, Nrf2, GSS, and SOD2 and down-regulated the expression of KEAP1 in a dose-dependent manner with p < 0.01 in Dio 80 or Dio 40 groups (the results of statistical analysis are provided in Supplemental Figure 2A–B).

Effects of dioscin on inflammatory signaling pathway. With regard to the inflammatory-related proteins, dioscin treatment significantly

Table 2 | The effects of dioscin on the biochemical parameters in C57BL/6J mice

Parameters	Control	HFD	HFD + Dio80	HFD + Dio40	HFD + Dio20	HFD + Sil
AST (IU/L)	13.23 ± 3.64**	58.57 ± 8.44	22.07 ± 6.08**	33.61 ± 7.63**	42.97 ± 9.97**	32.06 ± 7.03**
ALT (IU/L)	26.91 ± 4.94**	59.14 ± 5.46	22.32 ± 3.77**	26.67 ± 4.59**	43.13 ± 6.75**	40.57 ± 7.16**
Insulin (mIU/L)	15.81 ± 3.07**	27.67 ± 2.46	17.63 ± 2.56**	21.17 ± 2.01*	24.16 ± 2.59*	21.83 ± 3.37*
FFA (μmol/gprot)	39.79 ± 11.92**	120.51 ± 31.97	50.18 ± 12.01**	60.97 ± 17.44**	79.46 ± 21.11**	68.20 ± 20.04**
TC (mmol/L)	8.48 ± 2.71**	53.73 ± 9.21	10.44 ± 4.08**	22.73 ± 4.25**	34.48 ± 4.21**	21.02 ± 5.60**
TG (mmol/L)	128.89 ± 32.08**	233.94 ± 65.91	136.81 ± 39.08**	160.05 ± 53.87**	196.35 ± 57.57	166.18 ± 59.12*
MDA (U/mgprot)	15.85 ± 3.62**	75.83 ± 7.26	21.06 ± 4.19**	27.01 ± 4.59**	33.12 ± 4.30**	24.41 ± 3.29**
GSH (U/mgprot)	238.71 ± 8.21*	140.71 ± 29.5	206.29 ± 14.65*	199.11 ± 18.39	176.67 ± 10.15	182.99 ± 14.48
SOD (U/mgprot)	22.68 ± 6.88**	12.87 ± 2.82	20.43 ± 5.16**	16.40 ± 4.13**	13.70 ± 4.03**	16.91 ± 3.07**

Data are presented as mean ± SD (n = 8). *p < 0.05, **p < 0.01 compared with model group.



down-regulated the expression of AP-1, CYP2E1, COX-2, NF- κ B, and HMGB1 and up-regulated the I κ B- α expression compared with the model groups (the results of statistical analysis are provided in Supplemental Figure 2C–D). The livers from model mice exhibited drastically increased hepatic mRNA expression of TNF- α , IL-1, and IL-6, which all significantly decreased 2.42-, 2.35-, and 2.49-fold in ob/ob mice and 1.29-, 1.19-, and 1.09-fold in C57BL/6J model mice, respectively, upon dioscin 80 mg/kg treatment (Figure 3B–D).

Effects of dioscin on the MAPK signaling pathway. As shown in Figure 4A–D, the ob/ob group had high p-p38, p-ERK, and p-JNK levels which were all decreased by dioscin (80 mg/kg) with significance $p < 0.01$. And the HFD feeding increased hepatic p-p38, p-ERK, and p-JNK levels. Compared with model groups, the phosphorylation levels of p-p38, p-ERK, and p-JNK C57BL/6J mice were significantly down-regulated upon treatment with dioscin (80, 40, 20 mg/kg) in a dose-dependent manner with $p < 0.01$ in Dio 80 or Dio 40 groups.

Effects of dioscin on the autophagy pathway. As shown in Figure 5A–B, TEM assays revealed the ultrastructural conditions in ob/ob and C57BL/6 mice. Compared with the model groups, the number of lipid droplets obviously decreased upon dioscin treatment. More importantly, the compound induced macroautophagy as indicated by the red arrows. Next, the effects of dioscin on the expression of various autophagy-related proteins,

including p-mTOR/mTOR, LC3-II/GAPDH, Beclin1, and Atg5 were assessed, and the results indicated that dioscin significantly up-regulated their expression, especially dioscin 80 mg/kg with $p < 0.01$ (Figure 5C–D).

Effects of dioscin on fatty acid synthesis and metabolism. As shown in Figure 6A, the expression of ACADM, PPAR α , ACADS, ACSL1, and ACSL5 all decreased in ob/ob and HFD mice, which were significantly up-regulated by dioscin (80 mg/kg). The expression of LXR α was significantly down-regulated by dioscin (80, 40, 20 mg/kg) in a dose-dependent manner with $p < 0.01$ (the results of statistical analysis are provided in Supplemental Figure 3A–B). In addition, the mRNA levels of SREBP-1C, FAS, ACC1, SCD1 were significantly increased and meanwhile the CPT-1 and ACO were decreased in the livers of ob/ob and HFD-induced mice compared with the control groups. By contrast, dioscin supplementation significantly decreased the mRNA levels of SREBP-1C, FAS, ACC1, SCD1 and increased the CPT-1 and ACO of the genes in a dose-dependent manner with $p < 0.01$ in Dio 80 or Dio 40 groups (Figure 6B–C).

Effects of dioscin on TG and TC synthesis. As presented in Figure 6D, the expression of HMGCR, HMGCS1, and SREBP-2 were markedly up-regulated, and the expression of GPAT was significantly down-regulated by dioscin in a dose-dependent manner compared with the model groups in the livers of ob/ob

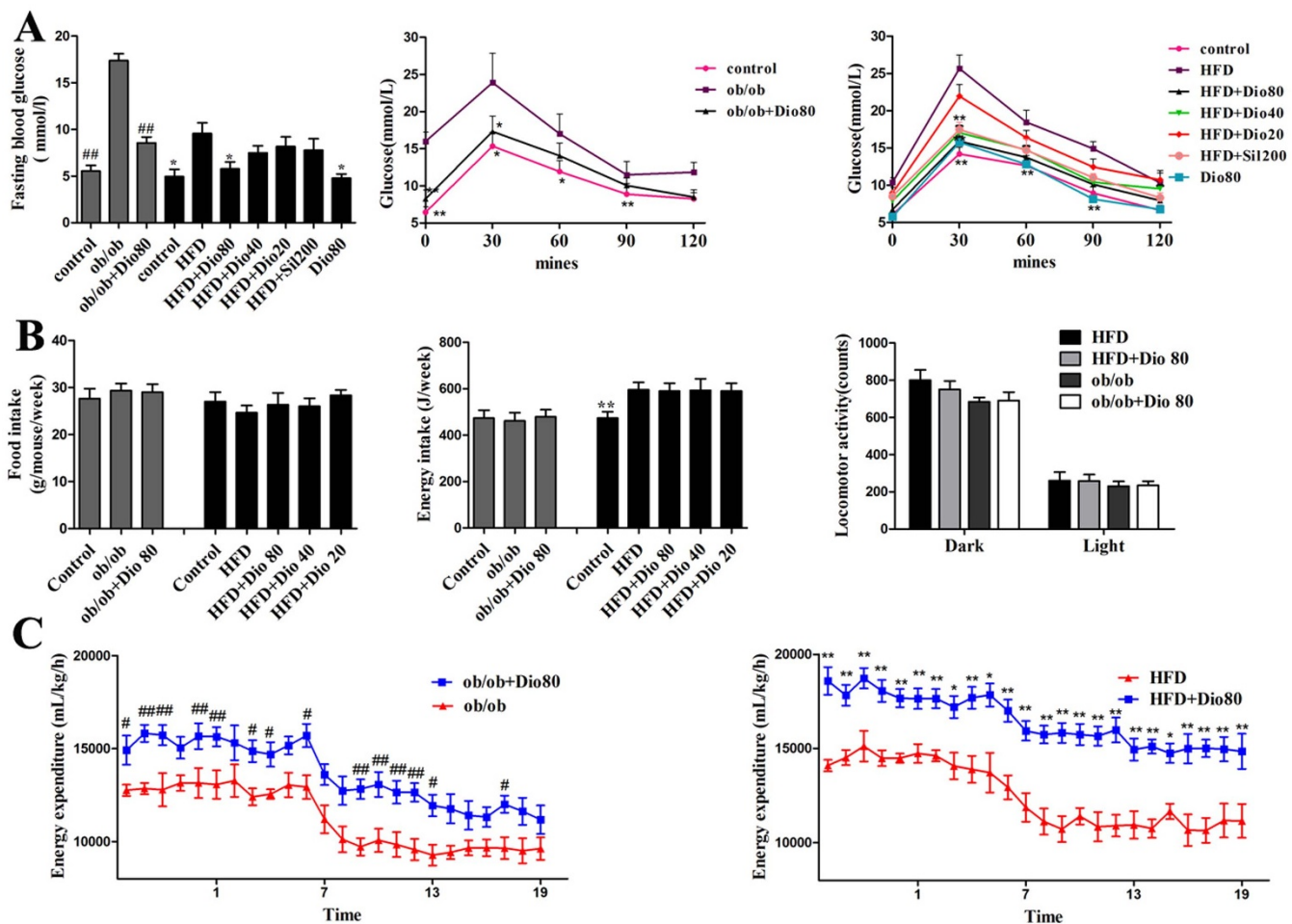


Figure 2 | Effects of dioscin on the OGTT and energy expenditure. Effects of dioscin on the fasting blood glucose levels and OGTT (A) in ob/ob and HFD-treated mice. Effects of dioscin on food intake, energy intake, locomotor activity (B) in ob/ob and HFD-treated mice. Effects of dioscin on energy expenditure (C) in ob/ob and HFD-treated mice. Indirect calorimetry measurements were done at day 60. Data are presented as mean \pm SD ($n = 8$). $^{\#}p, ^{*}p < 0.05$ and $^{##}p, ^{**}p < 0.01$ compared with model group.

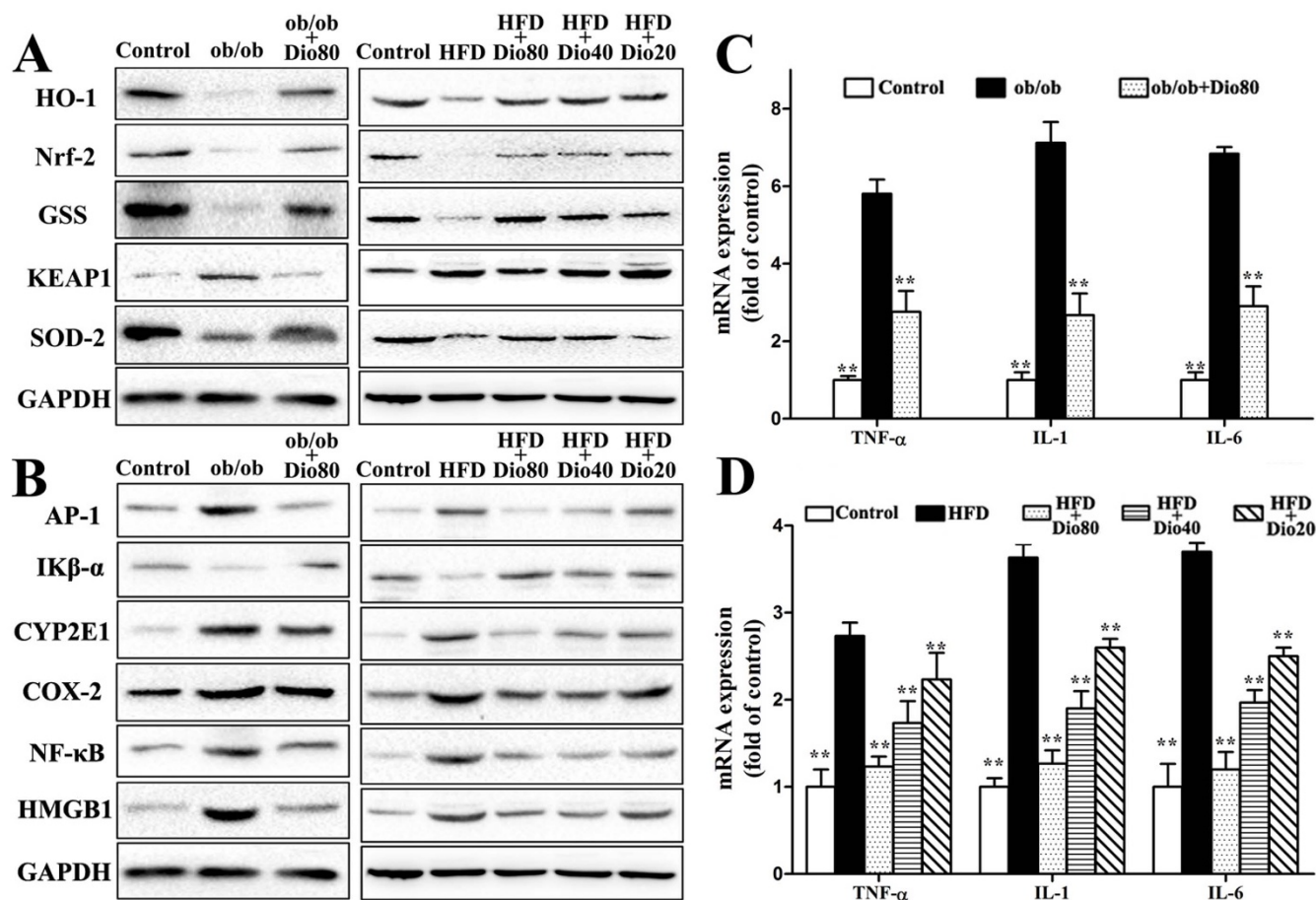


Figure 3 | Effects of dioscin on oxidative stress and inflammation in mice. Effects of dioscin on the expression of proteins related to oxidative stress, including HO-1, Nrf2, GSS, KEAP1, and SOD-2 (A). Effects of dioscin on the expression of proteins related to liver inflammation, including AP-1, IK β - α , CYP2E1, COX-2, NF- κ B, and HMGB1 (B). The cropped gels are used and full-length gels are presented in Supplementary Figure S4 and S5. Effects of dioscin on the expression of TNF- α , IL-1, and IL-6 (C and D). Data are presented as the mean \pm SD (n = 3). * p < 0.05 and ** p < 0.01 compared with the model group.

and HFD-induced mice (the results of statistical analysis are provided in Supplemental Figure 3C–D). In addition, DGAT1 and DGAT2 mRNA levels were also significantly down-regulated by the compound compared with the model groups with p < 0.01 in Dio 80 or Dio 40 groups (Figure 6E–F).

Discussion

Obesity is a multifactorial and complex condition featured by long-term intake of excess energy above energy consumption²⁶, which is a major harmful factor for numerous diseases. Consumption of high levels of dietary fat can cause obesity²⁷ and NAFLD²⁸. Thus, the development of new drugs for obesity and NAFLD therapy is necessary. In this study, ob/ob mice and HFD-induced C57BL/6J mice were used as the NAFLD models to prove the beneficial effects of dioscin. The results indicated that the levels of ALT, AST, FFA, TC, TG, MDA, GSH and SOD, as well as classic histopathological features were all ameliorated by dioscin. In addition, dioscin also evoked weight loss by increasing oxygen consumption and energy expenditure without inhibiting appetite or increasing physical activity in diet-induced and born obese mice. This agent should be developed as a new candidate for obesity and NAFLD prevention.

Mice with diet-induced NAFLD were characterized by obesity and impaired glucose metabolism²⁹ via body weight change, fasting glucose, OGTT and HFD-fed mice displayed metabolic syndromes. Therefore, in view of the high prevalence of abnormal glucose tolerance after an OGTT, an early intervention for NAFLD disease with

impaired fasting glucose and impaired glucose tolerance to prevent progression and hepatic fibrosis is needed.

Normal ROS levels are important to maintain various cellular functions. However, excessive ROS levels that surpass the capacity of the antioxidant system can cause oxidative stress³⁰, thereby leading to the peroxidation of membrane lipids and ultimately resulting in the production of MDA. In the present study, dioscin ameliorated the levels of MDA, GSH and SOD in ob/ob and HFD-induced C57BL/6J mice to inhibit oxidative stress. SOD2 catalyzes the dismutation of superoxide to hydrogen peroxide and molecular oxygen and reduces the risk of hydroxyl radical formation³¹. HO-1, an enzyme induced by heme, protects the liver from oxidative stress³² and Nrf2 affects HO-1 induction³³. KEAP1, a negative regulator of Nrf2, mediates Nrf2 degradation³⁴. In this study, down-regulated hepatic HO-1, Nrf2, and SOD2 as well as up-regulated KEAP1 were observed in the model groups, and these levels were all reversed by dioscin. These findings indicated that the effects of dioscin against NAFLD may be mediated by inhibiting oxidative stress.

NF- κ B is an important transcription factor that participates in the inflammatory reaction³⁵, whereas inhibition of the IK β - α kinase complex leads to inhibition of NF- κ B activation. Furthermore, CYP2E1 and oxidative stress generate ROS, which promote NF- κ B activation as well as ERK and p38 MAPK phosphorylation³⁶. In addition, the activities of NF- κ B and MAPK can cause increased expression of inflammatory cytokines³⁷. Pro-inflammatory mediators, including TNF- α , IL-6, NF- κ B, COX-2, HMGB-1 and AP-1, are

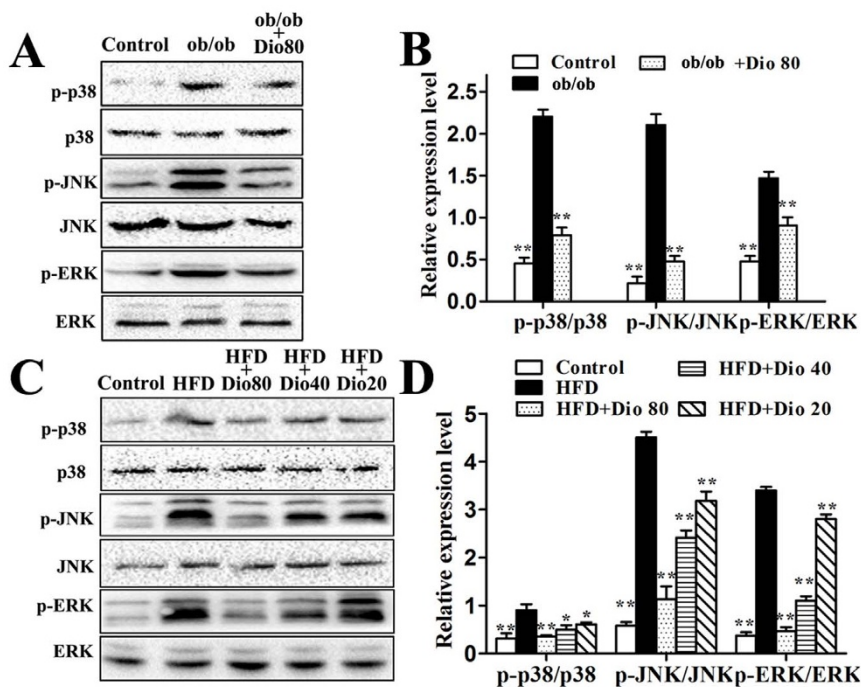


Figure 4 | Effects of dioscin on MAPK phosphorylation levels in ob/ob and C57BL/6J mice. The cropped gels are used and full-length gels are presented in Supplementary Figure S6 and S7. Data are presented as the mean \pm SD ($n = 3$). * $p < 0.05$ and ** $p < 0.01$ compared with the model group.

related with inflammatory diseases. In addition, emerging evidence links a chronic, slightly inflammatory state as well as chronic oxidative stress to the complex conditions of obesity, insulin resistance, and metabolic syndrome³⁸. The present study indicated that TNF- α , IL-1, IL-6, NF- κ B, COX-2, CYP2E1, HMGB-1 and AP-1 expression was up-regulated in ob/ob and HFD-treated C57BL/6J mice, and these levels were all reduced upon dioscin treatment. These findings suggest that the protective effect of dioscin against NAFLD may be mediated by decreasing hepatic inflammation.

Hepatic injury includes mitochondrial function, endoplasmic reticulum (ER) and oxidative stress, JNK and p38 activation, and macrophage accumulation before full progression into steatohepatitis. ERK1/2 MAPK involvement in the cellular response to oxidative stress has also been reported³⁹. In the present study, increased active levels of JNK and p38 as well as ERK1/2 phosphorylation levels were all reversed by dioscin compared with model groups. These results suggest that the protective effect of dioscin against NAFLD may be mediated by affecting MAPK phosphorylation levels.

Autophagy, an intracellular degradation pathway, is essential for energy and cellular homeostasis, which is regulated by mTOR dependent or mTOR-independent pathways⁴⁰. Current evidence demonstrates that NAFLD evolution is related to reduced autophagy function⁴¹. Our present study provided evidence of autophagosomes induced by dioscin based on TEN assays, and p-mTOR, Beclin1, Atg5, and LC3 expression was up-regulated by the chemical. These findings indicated that the protective effect of dioscin against NAFLD may be through the induction of autophagy, which should be considered as a novel approach for alleviating NAFLD liver conditions.

When fatty acid anabolism exceeds fatty acid catabolism, liver steatosis occurs⁴², which is characterized by an increased TG concentration. Upon SREBP-1c pathway inhibition, increased TG concentrations result from increased lipogenesis in the liver⁴³. In the progression of fatty acid synthesis, SREBP-1c plays an important role in regulation of gene transcription, including FAS, ACC1, and SCD1⁴⁴. LXR α belongs to the nuclear hormone receptor family and enhances the expression of lipogenic genes, including SREBP-1c⁴⁵. In the present study, the expression of proteins and genes related to fatty

acid synthesis were investigated. Dioscin administration significantly decreased the expression of LXR α , SREBP-1c, FAS, ACC1, and SCD1. These findings indicated that the protective effect of dioscin against NAFLD may occur through suppression of lipid synthesis.

With regard to fatty acid β -oxidation, the key enzymes, including ACADM, CPT-1, and ACO, are transcriptionally regulated by PPAR- α . Of these enzymes, CPT-1 and ACADS are the key enzymes involved in the regulation of mitochondrial β -oxidation of long-chain fatty acids⁴⁶. PPAR- α is a nuclear hormone receptor, and PPAR- α activation mediates lipoprotein metabolism, increases the esterification of free fatty acids, and promotes mitochondrial fatty acid uptake and oxidation. Furthermore, PPAR- α is regarded as a central regulator of hepatic glucose and lipid metabolism as well as a key component in the development of lipid disorders⁴⁷. In addition, the activities of ACSL1 and ACSL5, which belong to the family of long-chain acyl-CoA synthetases, promote β -oxidation of not only fatty acids but also PPAR- α agonists. These enzymes affect fatty acid β -oxidation and fatty acid synthesis⁴⁸. In the present paper, the results indicated that dioscin treatment elevated the expression of PPAR- α , CPT-1, ACADM, and ACADS, thereby indicating that dioscin may provide a protective effect against NAFLD by regulating PPAR- α and fatty acid oxidation.

Liver steatosis accompanied with the accumulation of TG potentially accelerates the progression of hepatic injury⁴⁹, which is characterized by increased TG concentrations. Glycerol-3-phosphate acyltransferase is important for the first esterification step of glycerol-3-phosphate to monoacylglycerol⁵⁰. DGAT1 and DGAT2 are responsible for the last esterification step of diacylglycerol to triacylglycerol⁵¹. Our study revealed that dioscin obviously inhibited increased TG levels and down-regulated GPAT, DGAT1, and DGAT2 mRNA expression. These results indicated that the protective effect of dioscin against NAFLD may occur through its effects on TG biological synthesis.

Hepatic cholesterol concentration appears to be primarily regulated through modulation of LDL receptor (LDL-R) expression and de novo synthesis⁵². The transcription factor SREBP2 promotes the expression of LDL-R and enzymes involved in cholesterol synthesis,

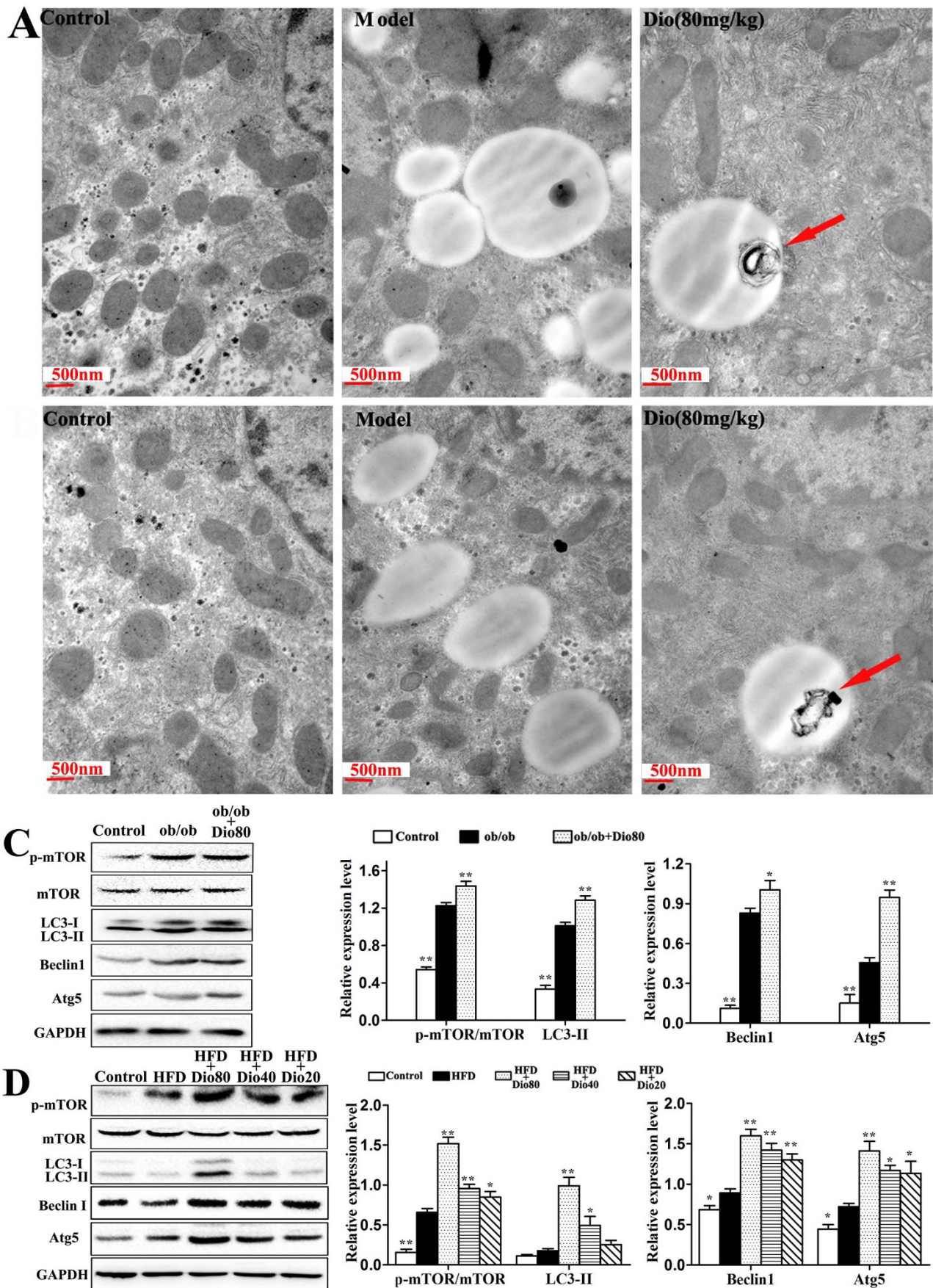


Figure 5 | Effects of dioscin on autophagy in mice. Effects of dioscin on macroautophagy in NAFLD liver using the TEM assay ($\times 25,000$, magnification) (A and B). Effects of dioscin on p-mTOR/mTOR, LC3 II, Beclin1, and Atg5 protein expression (C and D). The cropped gels are used and full-length gels are presented in Supplementary Figure S8 and S9. Data are presented as the mean \pm SD (n = 3). *p < 0.05 and **p < 0.01 compared with the model group.

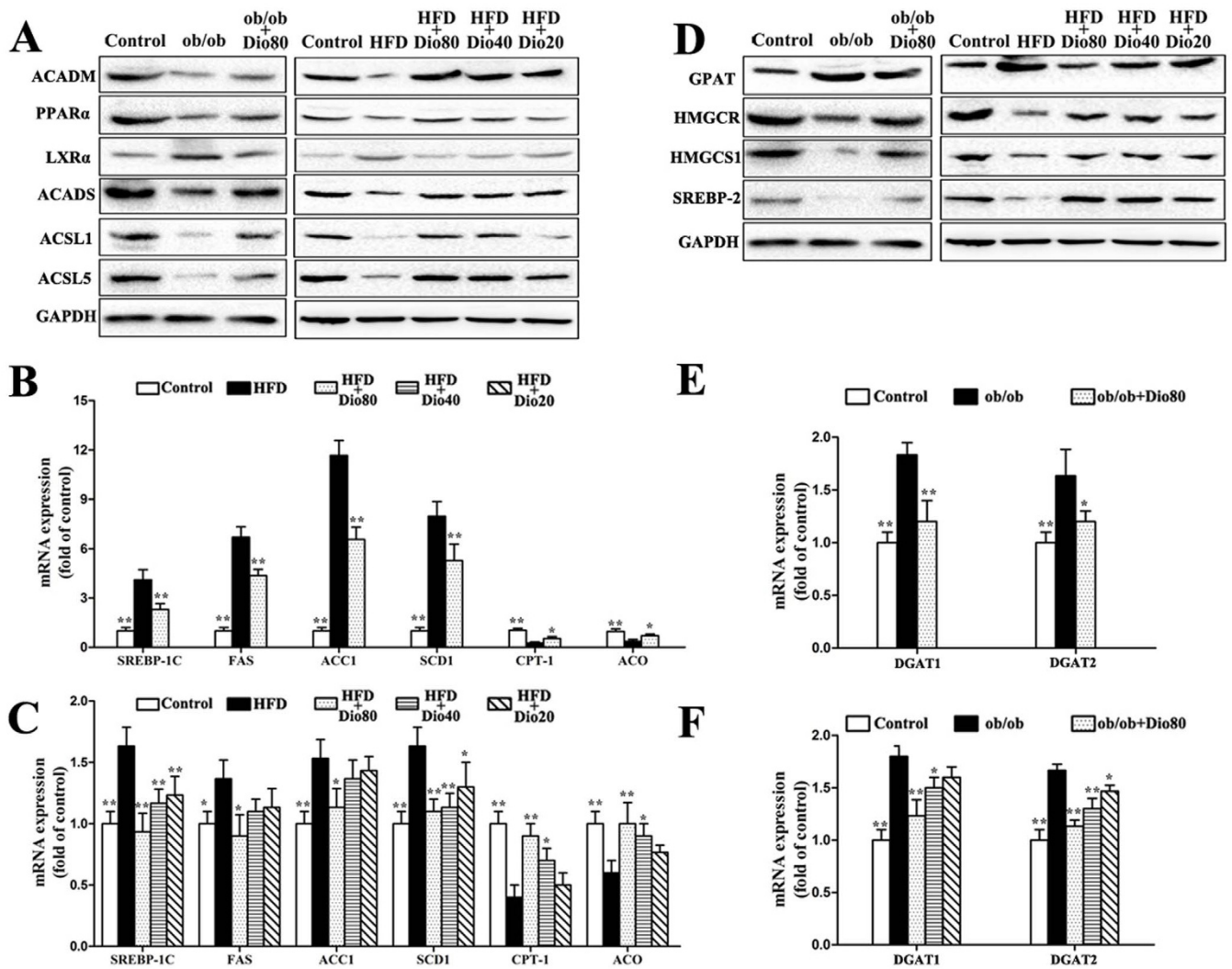


Figure 6 | Effects of dioscin on fatty acid synthesis and metabolism as well as TG and TC synthesis in mice. Effects of dioscin on the expression of ACADM, PPAR- α , LXR α , ACADS, ACSL1, and ACSL5 (A). Effects of dioscin on the mRNA expression of SREBP-1C, FAS, ACC1, SCD1, CPT-1, and ACO (B and C). Effects of dioscin on the expression of GPAT, HMGCR, HMGCS1, and SREBP-2 (D). The cropped gels are used and full-length gels are presented in Supplementary Figure S10 and S11. Effects of dioscin on DGAT1 and DGAT2 expression (E and F). Data are presented as the mean \pm SD (n = 3). *p < 0.05 and **p < 0.01 compared with the model group.

such as HMGCS and HMGCR⁵³. HMG-CoA is reduced to mevalonate (a precursor for cholesterol synthesis) by HMGCR and plays a critical role in production of LDL cholesterol as a rate-limiting enzyme in cholesterol biosynthetic pathway⁵⁴. SREBP2, HMGCS and HMGCR expression was increased in the dioscin treatment groups in the present study. These results indicated that the protective effect of dioscin against NAFLD may be mediated by its effects on TC biological synthesis.

The energy expenditure is closely related with the oxidation of fatty acids. And mitochondrial β -oxidation is the dominant oxidative pathway for fatty acids under normal physiological conditions. In the present work, dioscin significantly decreased fat accumulation in the liver, and markedly increased the expression of ACADM and UCP-1 to enhance the β -oxidation of fatty acid. Thus, we speculate that dioscin can decrease fat accumulation in the liver by inducing inefficient energy metabolism, e.g., by increasing UCP expression^{55,56}. The effective dose of dioscin may differ depending on physiologic parameters, and the physiological relevance of the supplied dose of the compound can improve the mitochondrial respiratory chain complex activities. Further studies are needed to explore the mechanisms of dioscin on energy expenditure in diet-induced and born obese mice.

In this paper, we showed that dioscin could evoke gradual weight loss without inhibiting the appetite or increasing the physical activity of obese mice. And the oral administration of dioscin lowered blood lipid, ameliorated hepatic fat accumulation, and decreased hepatic cholesterol, fatty acid and triglyceride deposition through inhibiting fatty acid synthesis, promoting fatty acid β -oxidation together with resisting oxidant stress, adjusting inflammation, regulating the MAPK signal pathway, and inducing autophagy. Consequently, we speculate that dioscin can induce the alterations in these liver metabolic pathways, which should be developed to be an efficient medication to treat obesity and obesity-related metabolic diseases in the future.

Methods

Animal experiments. Dioscin was prepared in our laboratory with the purity of over 98% analyzed by high-performance liquid chromatography (HPLC), and chemical structure of the compound was identified by MS and NMR^{18,57}, which was mixed in a solution of 0.5% carboxymethylcellulose sodium (CMC-Na) in distilled water. This solution was freshly prepared before administration everyday, and the dioscin was administered intragastrically (i.g.) at 80, 40 and 20 mg/kg once daily according to our previous work²⁴.

For the ob/ob mouse model, 5-week-old male ob/ob mice with the C57BL/6J genetic background and C57BL/6J mice were purchased from Nanjing University



(Nanjing, China). After 1 week of acclimatization, the mice were randomly divided into three groups: C57BL/6J lean littermates, ob/ob mice, and ob/ob mice treated with dioscin (80 mg/kg/day). After 8 weeks of feeding, the mice were sacrificed after an overnight fast. Then, blood and liver tissue were collected and stored for further analysis. For the HFD-induced mouse model, 5-week-old male C57BL/6J mice were purchased from Nanjing University (Nanjing, China). After 1 week of acclimatization, the mice were randomly divided into seven groups ($n = 10$ per group), including control group with a normal diet (control, 12% kcal fat content), model group with a high-fat diet (HFD, 45% kcal fat content), the mice fed a high-fat diet with a daily oral gavage of high-dose dioscin (80 mg/kg/day, HFD + Dio 80), the mice fed a high-fat diet with a daily oral gavage of medium-dose dioscin (40 mg/kg/day, HFD + Dio 40), the mice fed a high-fat diet with a daily oral gavage of low-dose dioscin (20 mg/kg/day, HFD + Dio 20), the mice fed a high-fat diet with a daily oral gavage of silymarin (20 mg/kg/day, HFD + Sil) and dioscin control with 80 mg/kg (Dio 80). The food intake in each group was detected once a week, and then the mean value of each mouse in different groups was calculated. The experimental diets were given *ad libitum* for 10 weeks in the form of pellets, and the mice were sacrificed after an overnight fast. Then, the blood and liver tissue were collected and stored for further analysis. All animals were housed in a controlled environment at $23 \pm 2^\circ\text{C}$ under a 12-hour dark/light cycle with free access to food and water. All experimental procedures were approved by the Animal Care and Use Committee of Dalian Medical University and performed in strict accordance with the People's Republic of China Legislation Regarding the Use and Care of Laboratory Animals.

Biochemical analysis. The serum parameters aspartate aminotransferase (AST), alanine aminotransferase (ALT), total triglyceride (TG), total cholesterol (TC), and liver tissue free fatty acid (FFA), superoxide dismutase (SOD), malondialdehyde (MDA) and glutathione (GSH) levels were detected using detection kits based on the manufacturer's instructions (Nanjing Jiancheng Institute of Biotechnology, Nanjing, China).

Oral glucose tolerance test (OGTT) and insulin levels. During the last week of treatment, oral glucose tolerance tests were performed. After fasting for 12 h, the mice were administered oral glucose (2 g/kg), and blood samples were obtained from the same main tail vein at 0, 30, 60, 90, and 120 min after glucose treatment. Blood glucose levels were tested using ACCU-CHEK touch test paper on an ACCU-CHEK Performa blood glucose meter (Roche Diagnostic, Mannheim, Germany). The concentration of insulin in serum was determined via a radioimmunity assay according to the kit's instructions using a ZC-2010 c-counter (USTC Chuangxin Co., Ltd., China).

Indirect calorimetry measurement. The animals were maintained in a comprehensive lab animal monitoring system (Oxymas/CLAMS, Columbus Instruments, Columbus, OH, USA) for 24 h, according to the manufacturer's instructions. Volume of O_2 consumption (VO_2 , mL/kg/h) and CO_2 production (VCO_2 , mL/kg/h), and physical activity were continuously recorded over a 24-h period. The respiratory exchange ratio (RER) was calculated as the ratio of carbon dioxide output to oxygen uptake (VCO_2/VO_2). Energy expenditure was calculated according to the following formula, provided by the manufacturer: energy expenditure = $(3.815 + 1.232\text{VCO}_2/\text{VO}_2) \times \text{VO}_2^{25}$.

Hepatic pathological evaluation. After being sacrificed, the liver tissues of the animals were embedded in paraffin and fixed in 10% formalin for at least 24 h. The samples were then cut into 5- μm pieces and fixed on slides according to the routine procedure. Liver sections were stained with hematoxylin and eosin (H&E), and the frozen sections of formalin-fixed livers were stained with Sudan III and Oil Red O. Then, the samples were analyzed by light microscopy (Nikon Eclipse TE2000-U, NIKON, Japan).

Transmission electron microscopy (TEM) assay. Fresh liver samples (3 mm \times 3 mm) obtained from the livers in control, model, and dioscin-treated groups (80 mg/kg) were fixed in 2% glutaraldehyde at 4°C for 24 h. Then, the regions of interest were excised with a glass scribe and fixed for ultramicrotomy. The sections were stained and observed using a transmission electron microscope (JEM-2000EX, JEDL, Japan).

Quantitative real-time PCR assay. Total RNA samples from livers were extracted using the RNAiso Plus reagent following the manufacturer's protocol. Reverse transcription for cDNA synthesis and quantitative real-time PCR analyses were performed as described⁵². The forward (F) and reverse (R) primers for the tested genes are presented in Supplemental Table 1. For each sample, the C_t values for the target gene and GAPDH (as a calibrator) were determined based on standard curves. The calculated relative C_t value of each gene was divided by the relative value of GAPDH. Then, the sample of each gene extracted from control group was set to one-fold and used to determine the relative values of other samples (n -fold).

Western blotting assay. Total proteins from livers were prepared using the tissue protein extraction kit (Bio-Rad, USA), and the obtained protein was measured using the Bradford Assay Kit (Bio-Rad, Hercules, CA). Protein samples were denatured by mixing with an equal volume of $2 \times$ sample loading buffer and boiling at 100°C for 5 min. Then, an aliquot (containing 50 μg protein) of the supernatant was loaded onto a SDS gel (8–12%), separated electrophoretically, and transferred to a PVDF

membrane (Millipore, USA). After the PVDF membrane was incubated with 10 mM TBS plus 1.0% Tween 20 and 5% dried skim milk (Boster Biological Technology, China) to block nonspecific protein binding, the membrane was incubated overnight at 4°C with primary antibodies (listed in Supplemental Table 2). Blots were then incubated with horseradish peroxidase-conjugated antibodies for 2 h at room temperature using a 1:2000 dilution (Beyotime Institute of Biotechnology, China). Protein expression was detected using an enhanced chemiluminescence (ECL) method and imaged by Bio-Spectrum Gel Imaging System (UVP, USA). To eliminate the variations due to protein quantity and quality, the data were adjusted to GAPDH expression (IOD of objective protein versus IOD of GAPDH protein). However, for the protein levels of MAPK phosphorylation, mTOR phosphorylation and LC3-II, the results were expressed as p-MAPK/MAPK, p-mTOR/mTOR, and LC3-II, respectively, following adjustments to GAPDH expression.

Statistical analysis. All data were evaluated as the mean and standard deviation (SD). Statistical analysis of the quantitative multiple group comparisons was performed using the one-way analysis of variance (ANOVA) followed by Duncan's test; whereas pairwise comparisons were performed using the t test by SPSS software (ver. 20.0; SPSS, Chicago, IL, USA). Results were considered to be statistically significant with $p < 0.05$.

- Mantena, S. K., King, A. L., Andringa, K. K., Eccleston, H. B. & Bailey, S. M. Mitochondrial dysfunction and oxidative stress in the pathogenesis of alcohol- and obesity-induced fatty liver diseases. *Free Radic Biol Med* **44**, 1259–1272 (2008).
- Smith, B. W. & Adams, L. A. Non-alcoholic fatty liver disease. *Crit Rev Clin Lab Sci* **48**, 97–113 (2011).
- Sanyal, A. J. *et al.* Nonalcoholic steatohepatitis: association of insulin resistance and mitochondrial abnormalities. *Gastroenterology* **120**, 1183–1192 (2001).
- Rolo, A. P., Teodoro, J. S. & Palmeira, C. M. Role of oxidative stress in the pathogenesis of nonalcoholic steatohepatitis. *Free Radic Biol Med* **52**, 59–69 (2012).
- Day, C. P. Non-alcoholic steatohepatitis (NASH): where are we now and where are we going? *Gut* **50**, 585–588 (2002).
- Zhang, H. F. *et al.* Protective effects of matrine against progression of high-fructose diet-induced steatohepatitis by enhancing antioxidant and anti-inflammatory defences involving Nrf2 translocation. *Food Chem Toxicol* **55**, 70–77 (2013).
- Cohen, J. I., Roychowdhury, S., DiBello, P. M., Jacobsen, D. W. & Nagy, L. E. Exogenous thioredoxin prevents ethanol-induced oxidative damage and apoptosis in mouse liver. *Hepatology* **49**, 1709–1717 (2009).
- Carter-Kent, C., Zein, N. N. & Feldstein, A. E. Cytokines in the pathogenesis of fatty liver and disease progression to steatohepatitis: implications for treatment. *Am J Gastroenterol* **103**, 1036–1042 (2008).
- Iacono, A., Raso, G. M., Canani, R. B., Calignano, A. & Meli, R. Probiotics as an emerging therapeutic strategy to treat NAFLD: focus on molecular and biochemical mechanisms. *J Nutr Biochem* **22**, 699–711 (2011).
- Homma, K., Suzuki, K. & Sugawara, H. The Autophagy Database: an all-inclusive information resource on autophagy that provides nourishment for research. *Nucleic Acids Res* **39**, D986–990 (2011).
- Mizushima, N., Levine, B., Cuervo, A. M. & Klionsky, D. J. Autophagy fights disease through cellular self-digestion. *Nature* **451**, 1069–1075 (2008).
- Sahini, N. & Borlak, J. Recent insights into the molecular pathophysiology of lipid droplet formation in hepatocytes. *Prog Lipid Res* **54**, 86–112 (2014).
- Xiong, Y. *et al.* Tectoridin, an isoflavone glycoside from the flower of *Pueraria lobata*, prevents acute ethanol-induced liver steatosis in mice. *Toxicology* **276**, 64–72 (2010).
- Yang, M. Y. *et al.* The hypolipidemic effect of *Hibiscus sabdariffa* polyphenols via inhibiting lipogenesis and promoting hepatic lipid clearance. *J Agric Food Chem* **58**, 850–859 (2010).
- Collier, J. Non-alcoholic fatty liver disease. *Medicine* **35**, 86–88 (2007).
- Balunas, M. J. & Kinghorn, A. D. Drug discovery from medicinal plants. *Life Sci* **78**, 431–441 (2005).
- Chang, C. J., Tzeng, T. F., Liou, S. S., Chang, Y. S. & Liu, I. M. Regulation of lipid disorders by ethanol extracts from *Zingiber zerumbet* in high-fat diet-induced rats. *Food Chem* **132**, 460–467 (2012).
- Yin, L. H. *et al.* An Economical method for isolation of dioscin from *Dioscorea nipponica* Makino by HSCCC coupled with ELSD, and a computer-aided UNIFAC mathematical model. *Chromatographia* **71**, 15–23 (2009).
- Hsieh, M. J., Tsai, T. L., Hsieh, Y. S., Wang, C. J. & Chiou, H. L. Dioscin-induced autophagy mitigates cell apoptosis through modulation of PI3K/Akt and ERK and JNK signaling pathways in human lung cancer cell lines. *Arch Toxicol* **87**, 1927–1937 (2013).
- Li, H. *et al.* Anti-thrombotic activity and chemical characterization of steroidal saponins from *Dioscorea zingiberensis* C.H. Wright. *Fitoterapia* **81**, 1147–1156 (2010).
- Li, M., Han, X. & Yu, B. Synthesis of monomethylated dioscin derivatives and their antitumor activities. *Carbohydr Res* **338**, 117–121 (2003).
- Lu, B. N. *et al.* Mechanism investigation of dioscin against CCl_4 -induced acute liver damage in mice. *Environ Toxicol Pharmacol* **34**, 127–135 (2012).



23. Zhao, X. M. *et al.* Dioscin, a natural steroid saponin, shows remarkable protective effect against acetaminophen-induced liver damage *in vitro* and *in vivo*. *Toxicol Lett* **214**, 69–80 (2012).
24. Xu, T. T. *et al.* Protective effects of dioscin against alcohol-induced liver injury. *Arch Toxicol* **88**, 739–753 (2014).
25. Xu, L. N. *et al.* iTRAQ-based proteomics for studying the effects of dioscin against nonalcoholic fatty liver disease in rats. *RSC Adv* **4**, 30704–30711 (2014).
26. Fukuda-Tsuru, S., Kakimoto, T., Utsumi, H., Kiuchi, S. & Ishii, S. The novel dipeptidyl peptidase-4 inhibitor teneliglipin prevents high-fat diet-induced obesity accompanied with increased energy expenditure in mice. *Eur J Pharmacol* **723**, 207–214 (2014).
27. Matsuzawa, Y. The metabolic syndrome and adipocytokines. *FEBS Lett* **580**, 2917–2921 (2006).
28. Kumashiro, N. *et al.* Cellular mechanism of insulin resistance in nonalcoholic fatty liver disease. *Proc Natl Acad Sci USA* **108**, 16381–16385 (2011).
29. Fabbrini, E., Sullivan, S. & Klein, S. Obesity and nonalcoholic fatty liver disease: Biochemical, metabolic, and clinical implications. *Hepatology* **51**, 679–689 (2010).
30. Cao, K. *et al.* Hydroxytyrosol prevents diet-induced metabolic syndrome and attenuates mitochondrial abnormalities in obese mice. *Free Radic Biol Med* **67**, 396–407 (2014).
31. Coyle, J. T. & Puttfarcken, P. Oxidative stress, glutamate, and neurodegenerative disorders. *Science* **262**, 689–695 (1993).
32. Takahashi, T., Morita, K., Akagi, R. & Sassa, S. Heme oxygenase-1: a novel therapeutic target in oxidative tissue injuries. *Curr Med Chem* **11**, 1545–1561 (2004).
33. McNally, S. J., Harrison, E. M., Ross, J. A., Garden, O. J. & Wigmore, S. J. Curcumin induces heme oxygenase 1 through generation of reactive oxygen species, p38 activation and phosphatase inhibition. *Int J Mol Med* **19**, 165–172 (2007).
34. McMahon, M., Itoh, K., Yamamoto, M. & Hayes, J. D. Keap1-dependent proteasomal degradation of transcription factor Nrf2 contributes to the negative regulation of antioxidant response element-driven gene expression. *J Biol Chem* **278**, 21592–21600 (2003).
35. Zhao, Y., Fu, Y., Hu, J., Liu, Y. & Yin, X. The effect of tissue factor pathway inhibitor on the expression of monocyte chemoattractant protein-3 and IkappaB-alpha stimulated by tumour necrosis factor-alpha in cultured vascular smooth muscle cells. *Arch Cardiovasc Dis* **106**, 4–11 (2013).
36. Mandrekar, P. & Szabo, G. Signalling pathways in alcohol-induced liver inflammation. *J Hepatol* **50**, 1258–1266 (2009).
37. Gao, B. & Bataller, R. Alcoholic liver disease: pathogenesis and new therapeutic targets. *Gastroenterology* **141**, 1572–1585 (2011).
38. Houstis, N., Rosen, E. D. & Lander, E. S. Reactive oxygen species have a causal role in multiple forms of insulin resistance. *Nature* **440**, 944–948 (2006).
39. Czaja, M. J., Liu, H. & Wang, Y. Oxidant-induced hepatocyte injury from menadione is regulated by ERK and AP-1 signaling. *Hepatology* **37**, 1405–1413 (2003).
40. Sarkar, S. Regulation of autophagy by mTOR-dependent and mTOR-independent pathways: autophagy dysfunction in neurodegenerative diseases and therapeutic application of autophagy enhancers. *Biochem Soc Trans* **41**, 1103–1130 (2013).
41. Yang, L., Li, P., Fu, S., Calay, E. S. & Hotamisligil, G. S. Defective hepatic autophagy in obesity promotes ER stress and causes insulin resistance. *Cell Metab* **11**, 467–478 (2010).
42. Musso, G., Gambino, R. & Cassader, M. Recent insights into hepatic lipid metabolism in non-alcoholic fatty liver disease (NAFLD). *Prog Lipid Res* **48**, 1–26 (2009).
43. Nakajima, T. *et al.* Peroxisome proliferator-activated receptor alpha protects against alcohol-induced liver damage. *Hepatology* **40**, 972–980 (2004).
44. Shimano, H. *et al.* Isoform 1c of sterol regulatory element binding protein is less active than isoform 1a in livers of transgenic mice and in cultured cells. *J Clin Invest* **99**, 846–854 (1997).
45. Lima-Cabello, E. *et al.* Enhanced expression of pro-inflammatory mediators and liver X-receptor-regulated lipogenic genes in non-alcoholic fatty liver disease and hepatitis C. *Clin Sci (Lond.)* **120**, 239–250 (2011).
46. Ramsay, R. R., Gandour, R. D. & van der Leij, F. R. Molecular enzymology of carnitine transfer and transport. *Biochim Biophys Acta* **1546**, 21–43 (2001).
47. Abdelmegeed, M. A. *et al.* PPARalpha expression protects male mice from high fat-induced nonalcoholic fatty liver. *J Nutr* **141**, 603–610 (2011).
48. Knight, B. L. *et al.* A role for PPARalpha in the control of SREBP activity and lipid synthesis in the liver. *Biochem J* **389**, 413–421 (2005).
49. Powell, E. E., Jonsson, J. R. & Clouston, A. D. Steatosis: co-factor in other liver diseases. *Hepatology* **42**, 5–13 (2005).
50. Butler, J. A., Hagen, T. M. & Moreau, R. Lipoic acid improves hypertriglyceridemia by stimulating triacylglycerol clearance and downregulating liver triacylglycerol secretion. *Arch Biochem Biophys* **485**, 63–71 (2009).
51. Gnoni, G. V., Paglialonga, G. & Siculella, L. Quercetin inhibits fatty acid and triacylglycerol synthesis in rat-liver cells. *Eur J Clin Invest* **39**, 761–768 (2009).
52. Zhang, S. *et al.* Effects of flavonoids from *Rosa laevigata* Michx fruit against high-fat diet-induced non-alcoholic fatty liver disease in rats. *Food Chem* **141**, 2108–2116 (2013).
53. Vallim, T. & Salter, A. M. Regulation of hepatic gene expression by saturated fatty acids. *Prostaglandins Leukot. Essent Fatty Acids* **82**, 211–218 (2010).
54. Martina, F., Klemen, Š., Uršula, P. & Damjana, R. High-fat Medium and Circadian Transcription Factors (Cryptochrome and Clock) Contribute to the Regulation of Cholesterogenic Cyp51 and Hmger Genes in Mouse Embryonic Fibroblasts. *Acta Chim Slov* **55**, 85–92 (2008).
55. Minokoshi, Y. *et al.* Leptin stimulates fatty-acid oxidation by activating AMP-activated protein kinase. *Nature* **415**, 339–343 (2002).
56. Lee, Y. M. *et al.* Effects of dietary genistein on hepatic lipid metabolism and mitochondrial function in mice fed high-fat diets. *Nutrition* **22**, 956–964 (2006).
57. Yin, L. H. *et al.* A green and efficient protocol for industrial-scale preparation of dioscin from *Dioscorea nipponica* Makino by two-step macroporous resin column chromatography. *Chem Eng J* **165**, 281–289 (2010).
58. Kim, M. *et al.* Anti-obesity effect of alpha-lipoic acid mediated by suppression of hypothalamic AMP-activated protein kinase. *Nat Med* **10**, 727–733 (2004).

Acknowledgments

This work was supported by the Doctorate in Higher Education Institutions of Ministry of Education (No. 20122105110004), the Program for Liaoning Innovative Research Team in University (LT2013019) and the Program for New Century Excellent Talents in University (NCET-11-1007).

Author contributions

M.L., L.X. and J.P. designed the experiments and wrote the main manuscript text; M.L. and L.Y. prepared the figures; M.L., Y.Q. and X.H. performed the animal experiments; M.L., Y.X., Y.Z. and H.S. performed the Real-time PCR and western blotting assays; Y.L., J.Y. and K.L. analyzed the data; J.P. overall supervised the conduct of the study. All authors reviewed the manuscript.

Additional information

Supplementary information accompanies this paper at <http://www.nature.com/scientificreports>

Competing financial interests: The authors declare no competing financial interests.

How to cite this article: Liu, M. *et al.* Potent effects of dioscin against obesity in mice. *Sci Rep.* **5**, 7973; DOI:10.1038/srep07973 (2015).



This work is licensed under a Creative Commons Attribution-NonCommercial-ShareAlike 4.0 International License. The images or other third party material in this article are included in the article's Creative Commons license, unless indicated otherwise in the credit line; if the material is not included under the Creative Commons license, users will need to obtain permission from the license holder in order to reproduce the material. To view a copy of this license, visit <http://creativecommons.org/licenses/by-nc-sa/4.0/>

SCIENTIFIC REPORTS

Corrigendum: Potent effects of dioscin against obesity in mice

Min Liu, Lina Xu, Lianhong Yin, Yan Qi, Youwei Xu, Xu Han, Yanyan Zhao, Huijun Sun, Jihong Yao, Yuan Lin, Kexin Liu & Jinyong Peng

Scientific Reports 5:7973; doi: 10.1038/srep07973; published online 22 January 2015; updated 17 July 2015

This Article contains an error in Fig. 1c: the Sudan III staining for the 'ob/ob' group is incorrect. The correct Fig. 1C appears below as Fig. 1.

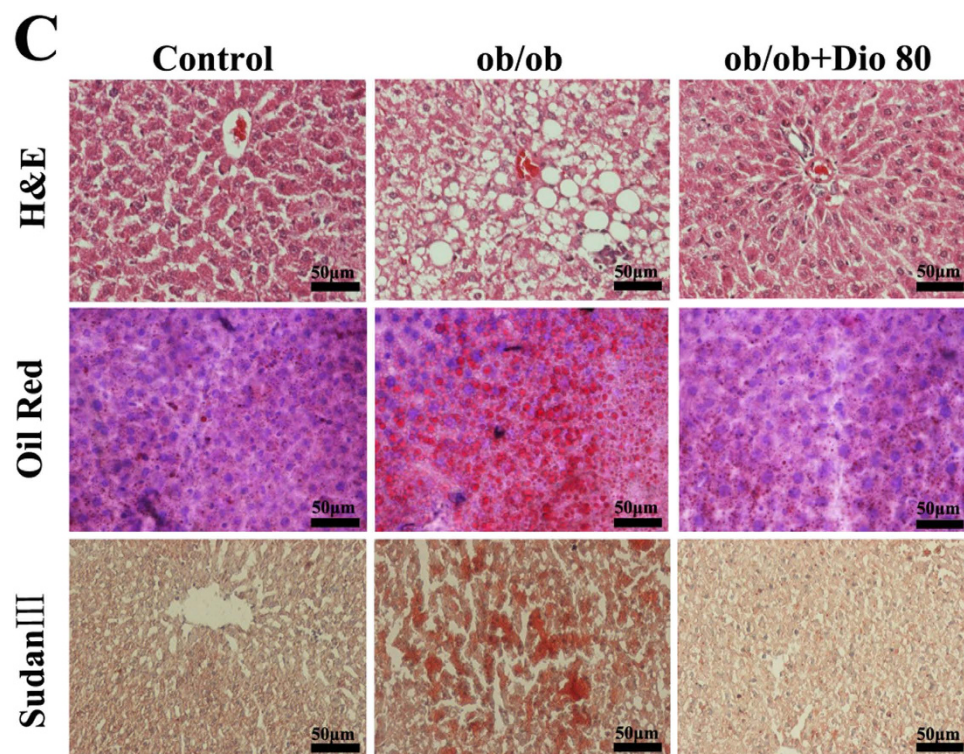


Figure 1.